Annals of the University of Craiova, Mathematics and Computer Science Series
Volume 46(2), 2019, Pages 426–432
ISSN: 1223-6934

Study and simulation of soil salinity evolution by Reflexw and GprMax

Ahmed Faize, Fouad Lahalal, and Mohamed Atounti

Abstract. Degradation of soil quality is a serious threat to the sustainability of irrigated systems. To prevent this degradation, it becomes necessary to develop simulation models to assess the long-term effects of road practices. The main purpose of this article is to simulate the salt signals taken by the GPR radar, using Reflexw and GprMax softwares. Note, however, that the operation of these two programs is based on numerical methods including finite difference method (FD) for Reflexw and finite difference time domain (FDTD) for GprMax. During the spread of radar signal in a geological environment, we note that the signal decreases because of the phenomenon of absorption and reflection, and we find that the physical setting that has a great influence on the conduct of the wave in different geological environments is the effective permittivity.

2010 Mathematics Subject Classification. 65L12; 35Q60.
Key words and phrases. GPR, Salinity, Electromagnetic Wave, FDTD.

1. Introduction

Soil salinization is one of the most common forms and drivers of land degradation, and entails significant environmental, social, and economic consequences. It is estimated that 20% of the total land area of Morocco is affected by salinity. With the rapidly increasing population densities and drastic land use changes over the past few decades, soil salinization has become the main restraint not only for a sustainable development of agriculture, but also for the stability of regional ecosystems. Timely detection as well as assessment of soil salinity are essential to regional ecological stability, and these problems have attracted considerable attention worldwide in recent years.

Ground penetrating radar (GPR) is a similar technique to the seismic imagery reflection [1]. It uses electromagnetic waves that propagate and refract in heterogeneous medium in order to scan, to localize and to identify quantitative variations within electric and magnetic proprieties of the soil. GPR uses an array of frequencies ranged from 10 MHz to 2.6 GHz. When using lower frequency antenna (between 10 and 100 MHz) investigated depth will be higher (more than 10 m), however resolution remains lower [2].

The treatment of geophysical data is based on numeric modeling of signals captured by the radar. Within electromagnetic field numeric modeling appeared at the beginning of the seventies [3] and coincided with the introduction of powerful and accessible microprocessors that allow realization of personal calculation within a short

Received November 28, 2018. Accepted November 15, 2019.
This paper has been presented at the Conference MOCASIM, Marrakesh, 26-27 November 2018.

time [4]. It is possible to model the physical proprieties implicated in any geophysical technique by using either forward modeling or inverse modeling. Forward modeling takes as model subsoil that includes all of its appropriate physical proprieties and uses theoretical equations in order to simulate the response of the receiver. This, in turn, will determine a given technique to measure through the model. However, reverse modeling uses data collected from the field in order to create a model of subsoil that will fit better with the original data. To obtain reliable data, a number of measures and data processing must be performed. Forward modeling allows us to test and to determine how proprieties of subsoil materials will change.

GPR is used for the exploration of the subsoil in several research fields such as the detection of landmines [5], geology [6, 11], civil engineering [7], glaciology [8, 9] and archeology [10]. It was also successfully applied to 2D imaging of cracks and fractures in resistive soils such as gneiss [12] [14]. In this work we intend to simulate the salt signals taken by the GPR radar, using Reflexw and GprMax software.

2. Theoretical background and method

2.1. GPR operating principle. GPR is a nondestructive method that has been proved for internal imaging of several types of geological materials such as granite and engineered materials such as concrete construction and other buried structures (pipes, cables ...). The signal can penetrate into the soil and into material buried within the soil, allowing its detection as well as its depth below the ground surface. The operating principles of various existing GPR radar are based on the same principle: a transmitting antenna is placed in contact with the ground, emitting short pulses towards the ground (Figure 1 (a) Tx). The electromagnetic wave generated propagates inside the ground that is considered as a dielectric medium. If an obstacle is encountered, a part of the signal emitted by the antenna of GPR returns to the soil surface (reflected wave) and then detected by the receiving antenna (Figure 1 (a) Rx). This recovered wave reflects a trace of subsoil at a specific point and at given time. As the user moves the GPR radar above the studied field, new signals are transmitted and reflected signals are again recovered at the receiving antenna. This process (sending and receiving generated signals) leads to the acquisition of a set of traces of soil, as numerical data, following a straight prospecting direction thereby establishing what it is called a radargram or a B-scan (Figure 1 (b)) of the studied medium. The treatment of the data set is provided by specialized software that allows the obtaining of hyperbola (Figure 1 (b)). Note that the hyperbola observed in this figure, is an extremely important index, since it gives, suitable information about localization of buried objects.

2.2. Description of soil salinity. The fundamental components of soils are mineral particles, organic matter, water and air. Mineral particles are inorganic materials derived from rocks by weathering. The pore space, organic matter and living organisms are filled with water and air. Soil water and air typically make up about 50% of the soil volume. The Soil salinity reduces plant growth and causes crop failure by limiting plant water uptake due to an osmotic effect making it more difficult for the plant to extract water, by specific-ion toxicity, or by upsetting the nutritional balance of plants. The volumetric effective relative dielectric constant can be described

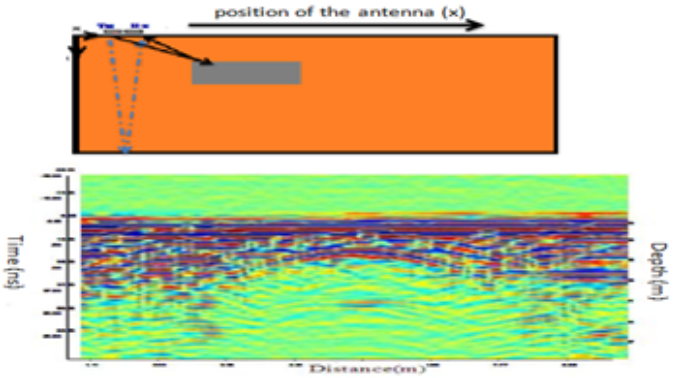

FIGURE 1. Schematic explanation of the principle of the GPR.

approximately as a mean value of all of the dielectric constants of the different soil components:

$$\varepsilon_{eff} \approx \sum_{i=1}^{n} \varepsilon_i \upsilon_i \tag{1}$$

where

- ε_{eff} : effective relative dielectric constant.
- ε_i : component dielectric constant.
- υ_i : component relative volume.
- n : number of soil components

2.3. FDTD based modeling and simulation. Maxwell's electromagnetic equations that mathematically express the relations between the fundamental electromagnetic field quantities and their dependence on their sources can be used to describe all electromagnetic phenomena. The fundamental equations are [15]: Acquisition methods have to be synchronized and all referred to the same coordinate system in order to integrate the geometric data collected by the different techniques [16]. To illustrate the application of finite differences centered to the Maxwell equations, take the case of Ampere equation in the 2D case in TM mode:

$$\varepsilon \frac{\partial E_z}{\partial t} + \sigma E_z = \frac{\partial Hy}{\partial x} - \frac{\partial Hx}{\partial y} \tag{2}$$

In (i, j) and time $n + \frac{1}{2}$, we have: This equation calculates the field E_z^{n+1} based on Fields E_z^n, $H_x^{n+\frac{1}{2}}$ and $H_y^{n+\frac{1}{2}}$. We proceed in the same manner for the expression of each component of the electromagnetic field. This discretization of Maxwell's equations constitutes the basis of the Yee algorithm as shown in Figure 2.

$$\begin{aligned} \varepsilon \frac{E_z|_{i,j}^{n+1} - E_z|_{i,j}^{n}}{dt} + \sigma \frac{E_z|_{i,j}^{n+1} - E_z|_{i,j}^{n}}{dt} = & \frac{H_y|_{i+\frac{1}{2},j}^{n+\frac{1}{2}} - H_y|_{i-\frac{1}{2},j}^{n+\frac{1}{2}}}{dx} \\ & - \frac{H_x|_{i,j+\frac{1}{2}}^{n+\frac{1}{2}} - H_x|_{i,j-\frac{1}{2}}^{n+\frac{1}{2}}}{dy} \end{aligned} \tag{3}$$

whether

$$E_z|_{i,j}^{n+1} = \frac{1-\frac{\sigma\cdot\partial t}{2\cdot\varepsilon}}{1+\frac{\sigma\cdot\partial t}{2\cdot\varepsilon}} E_z|_{i,j}^{n} + \frac{\frac{\partial t}{\varepsilon}}{1+\frac{\sigma\cdot\partial t}{2\cdot\varepsilon}} \left(\frac{H_y|_{i+\frac{1}{2},j}^{n+\frac{1}{2}} - H_y|_{i-\frac{1}{2},j}^{n+\frac{1}{2}}}{dx} - \frac{H_x|_{i,j+\frac{1}{2}}^{n+\frac{1}{2}} - H_x|_{i,j-\frac{1}{2}}^{n+\frac{1}{2}}}{dy} \right)$$

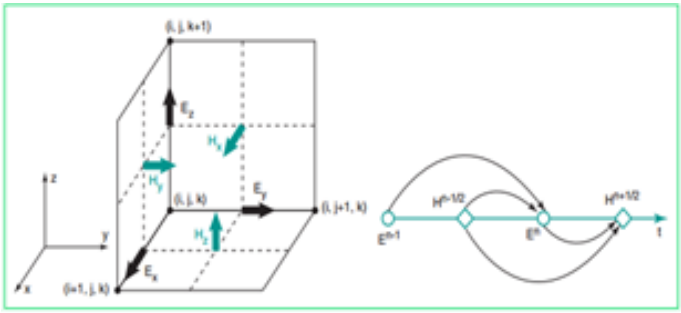

FIGURE 2. Yee cell in Cartesian coordinates.

3. Results

Simulate signals GPR, Reflexw and GPRmax require a number of parameters such as the frequency of the antenna used, the geometry of the ground, the dielectric permittivity, magnetic permeability and electrical conductivity of the media involved in the simulation. To the simulation, such as by Reflexw and GprMax, of the soil, in which the salt (rectangular or circular form) is buried, is simulated by wet soil whose dielectric properties $\varepsilon_r = 30$ and $\sigma = 0.16S/m$. The salt, *conductivity* $= 9.93.$ $10S/m$, is buried at a depth of $0.5m$ and is located at the surface, between 0.8 m and $1.2m$ along the Ox axis (Fig 4a and Fig 4b). Frequency simulation is set at $800MHz$. The emission and reflection of the simulated signal is recorded on a time window of $20ns$ with a spatial increment of $7cm$. Figure 3 (a,b) shows a geometric model of bar rectangular of salt used for simulation of radar signals reflected by a simulator (GprMax). The results obtained are summarized and represented by the software, as radargram as in Figure 3 (c,d) (by GprMax) and Figure 4 (c,d) by Reflexw. In these figures we note the presence of two diffraction hyperbolas that indicate the presence of the salts around $0.5m$, this is exactly the depth at which it was supposed to bury this bar.

4. Conclusion

GPR is not widely accepted as a method to measure subsurface soil water content. However, in recent years, GPR instrumentation has seen intensive development, allowing faster, easier and most importantly, more accurate soil moisture content measurements. Hence, spatial resolution has improved, particularly for this application where the required penetration depth is low, so that small heterogeneities in the field

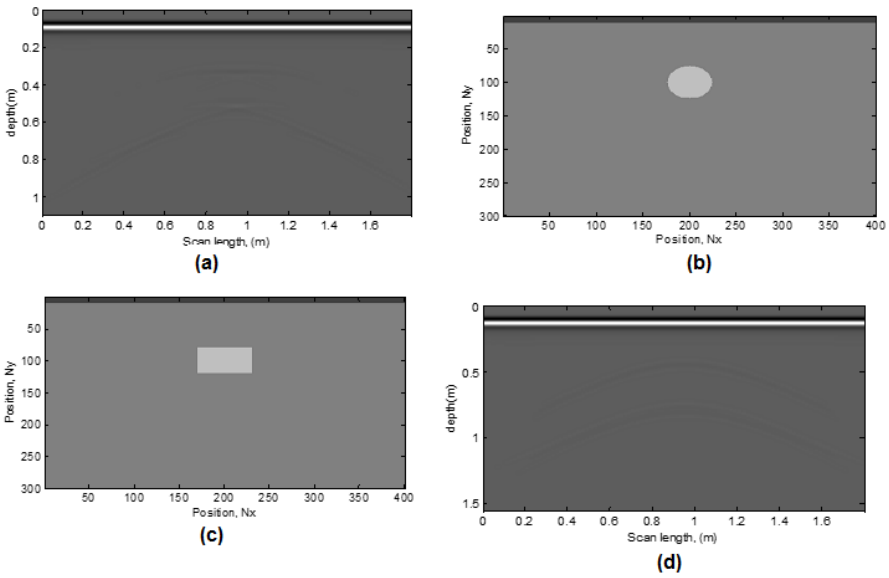

FIGURE 3. Diagram representing the position of the salts in the rectangular block (a) and circular block (b) by GprMax. Radargram the buried rectangular salts (c) and circular salts (d) in the wet sand for 800 MHz antenna.

can be used to obtain information on the relative permittivity and analyzed to calculate soil moisture content. We presented a GPR method to measure subsurface soil moisture content. This method currently relies on calibration tests in the laboratory and in the field for a better understanding of petrophysical property relations between permittivity and volumetric moisture content. Further studies are needed for more information on this issue. The simulation results we have achieved for different objects (salts rectangular and circular) buried, show that the detection of objects buried under ground, the radar GPR is through a process signal that leads to the production of radargrams where hyperbole that appear indicate the existence of these objects, while giving their exact locations in the soil depth. The change of the permittivity causes the reflection of the electromagnetic wave, while attenuates conductivity, more the permittivity of the dielectric perfect medium is high more the amplitude of the reflected wave increases. By against, most middle is the wave conductor tends to diminish.

References

[1] M. Bano, F. Pivot, J.M. Marthelot, Modeling and filtering of surface scattering in ground-penetrating radar waves, *First Break* 17 (1999), 215–222.

[2] D.A. Noon, G.F. Stickley, D. Longstaff, A frequency-independent characterization of GPR penetration and resolution performance, *Journal of Applied Geophysics* **40** (1998), 127–137.

[3] H.W. Chen, H. Tai-Min, Finite Difference Time Domain Simulation of GPR Data, *Journal of Applied Geophysics* **40** (1998), 139–163.

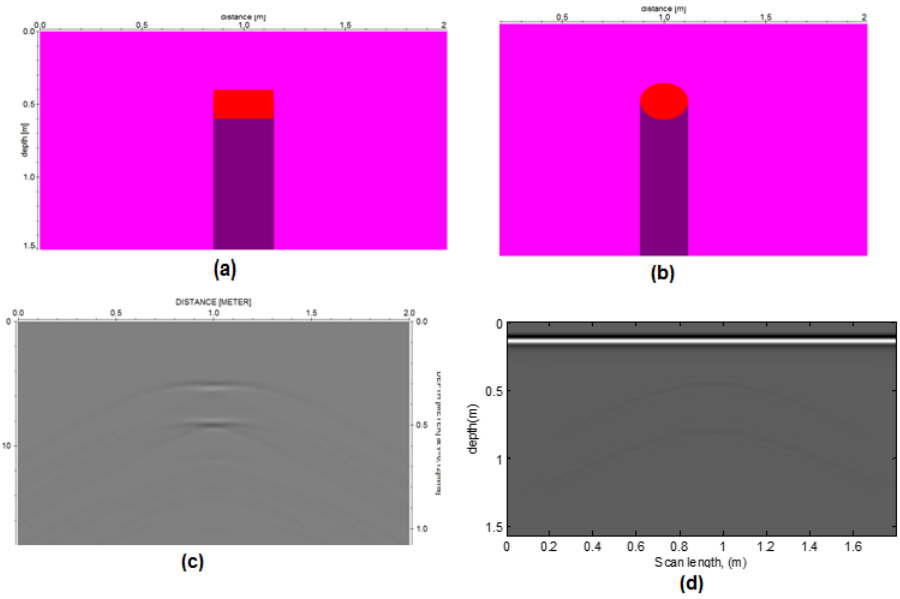

FIGURE 4. Diagram representing the position of the salts in the rectangular block (a) and circular block (b) by ReflexW. Radargram the buried rectangular salts (c) and circular salts (d) in the wet sand at a depth $0.5m$ for $800MHz$ antenna.

[4] E. Ceruzzi Paule, *A History of Modern Computing History of Computing*, MIT Press, Cambridge, Massachusetts, 1998, ISBN:0-262-03255-4

[5] A. Hamadi, Analyse et prdiction comportementales du radar GPR polarimtrique de la mission spatiale EXOMARS, Thse de Doctorat de l'Universit De Limoges, France, 2010.

[6] Z.W. Gu, The Application of Ground Penetrating Radar to Geological Investigation on Ground in Cold Regions, *Journal of Glaciology and Geocryology* **16** (1994), 283–289.

[7] C.P.F. Ulriksen, Application of impulse radar to civil engineering, PhD Thesis, Lund University of Technology, Lund, Sweden, 1982.

[8] F.J. Navarro, J.J. Lapazaran, F. Machio, C. Martin, J. Otero, On the Use of GPR Energetic Reflection coefficients in Glaciological Applications, *Geophysical Research* **11** (2009), EGU2009-9804, EGU General Assembly.

[9] J. Woodward, M.J. Burke, Applications of Ground-Penetrating Radar to Glacial and Frozen Materials, *Journal of environmental and engineering geophysics* **12** (2007), 69–85.

[10] J. Leckebusch, Ground-Penetrating Radar: A Modern Three-dimensional Prospection Method, *Archaeological Prospection* **10** (2003), 213–240.

[11] A.K. Benson, Application of ground penetrating radar in assessing some geological Hazards: examples of ground water contamination, faults, cavities, *Journal of Applied Geophysics* **33** (1995), 177–193.

[12] M. Grasmueck, 3-D Ground-penetrating radar applied to fracture imaging in gneiss, *Geophysics*, **61** (1996), 1050–1064.

[13] A. Giannopoulos, *GprMax2D3D, User's Guide*, 2005, http://www.gprmax.org; http://www.gprmax.org

[14] U. Basson, I. Gev, Z. Ben-Avraham, Mapping shallow stratigraphy of dunes and moisture content with a ground penetrating radar, *Israel Geological Society annual meeting* **3** (1992), 17.

[15] D. De Domenico, A. Teramo, FDTD modelling in high-resolution 2D and 3D GPR surveys on a reinforced concrete column in a double wall of hollow bricks, *Near Surface Geophysics*, **11** (2013), 29–40.
[16] B. Lampe, Finite-Difference Time-Domain Modeling of Ground-Penetrating Radar Antenna Systems, DISS. ETH NO. 15261, 2003.

(Ahmed Faize, Fouad Lahalel, Mohamed Atounti) Laboratory of Applied Mathematics and Information Systems, Multidisciplinary Faculty of Nador, University of Mohammed First, 62702 Selouane-Nador, Morocco
E-mail address: ahmedfaize6@hotmail.com, fpn.lahlal@gmail.com, atounti@hotmail.fr